Polyhedron 168 (2019) 72–79

Contents lists available at ScienceDirect

Polyhedron

journal homepage: www.elsevier.com/locate/poly

Rare-earth complexes of the asymmetric amide ligands, $N(SiMe_3)Ph$ and $N(SiMe_3)Cy$

Samuel A. Moehring, Joseph W. Ziller, William J. Evans *

Department of Chemistry, University of California, Irvine, CA 92697-2025, United States

ARTICLE INFO

Article history:
Received 22 December 2018
Accepted 18 April 2019
Available online 27 April 2019

Keywords:
Rare-earth metals
Amide ligands
Lanthanides
Steric saturation
Triflates

ABSTRACT

Salt metatheses of the rare-earth metal triflates, $Ln(OTf)_3$ (Ln = Sc, Y, La, Ce, Pr, Gd, Dy, Ho, Tb, Lu; OTf = SO_3CF_3), with $KN(SiMe_3)Ph$ in THF generate the $Ln[N(SiMe_3)Ph]_3(THF)$ complexes which were characterized by X-ray crystallography. All three phenyl substituents in the $Ln[N(SiMe_3)Ph]_3(THF)$ complexes are on the same side of the N_3 plane and form a pocket that surrounds the THF. $Y(OTf)_3$ and $Ho(OTf)_3$ react similarly with $LiN(SiMe_3)Cy$ to make the analogous $Ln[N(SiMe_3)Cy]_3(THF)$ complexes which were also crystallographically identified. The $Ln[N(SiMe_3)Cy]_3(THF)$ complexes display disorder in one ligand such that some molecules have three cyclohexyl groups on one side of the N_3 plane and others have two.

1. Introduction

Numerous complexes of rare-earth metals and amide ligands, NR_2, have been reported in the literature [1–3]. With small alkyl R groups like Me and Et, the $Ln(NR_2)_3$ complexes are typically insoluble in common solvents and with ^{i}Pr substituents, $\{Ln[N(^iPr)_2]_4\}^-$, "ate" salts can form [2,4–8]. The bis(trimethylsilyl) amide ligand originally introduced by Bradley, $N(SiMe_3)_2$ [9–11], and the dimethylsilyl analog, $N(SiHMe_2)_2$ [12–14], developed by Anwander, are by far the most heavily investigated amides with the rare-earth metals. The syntheses of $Ln[N(SiMe_3)Ph]_3(THF)_x$ complexes (Ln = Y, La, Nd, Sm, Eu, Tb, Dy, Er, Yb, Lu, x = 0–2) from $LnCl_3$ and $LiN(SiMe_3)Ph$ were reported in 1995, but $Nd[N(SiMe_3)Ph]_3(THF)$ was the only example that was fully defined by X-ray crystallography [15].

In efforts to expand the synthetic and structural chemistry of tris(amide) rare-earth metal amides available for studies of reductive chemistry [16–18], rare-earth metal triflate precursors have been used to synthesize complexes with $N(SiMe_3)Ph$ [15] and $N(SiMe_3)Cy$ [19] ligands. The products were characterized by X-ray crystallography to generate a data base with which to evaluate steric factors using the solid angle G parameter of Guzei [20] which has proven useful in reductive chemistry [21] and in rare earth metal amide chemistry [22]. To our knowledge, complexes of $N(SiMe_3)Cy$ ligands with the rare-earth metals have not been reported previously.

2. Results

2.1. $Ln[N(SiMe_3)Ph]_3(THF)$ complexes

Rare-earth metal triflates were investigated as precursors alternative to the common lanthanide chlorides. The ionic metathesis reactions of $Ln(OTf)_3$ with $KN(SiMe_3)Ph$ in THF generate the complexes $Ln[N(SiMe_3)Ph]_3(THF)$, **1-Ln**, as shown in Eq. (1). The diamagnetic complexes of Sc, Y, La, and Lu gave unexceptional ^1H and $^{13}C\{^1H\}$ NMR spectra.

* Corresponding author.
E-mail address: wevans@uci.edu (W.J. Evans).

https://doi.org/10.1016/j.poly.2019.04.026
0277-5387/

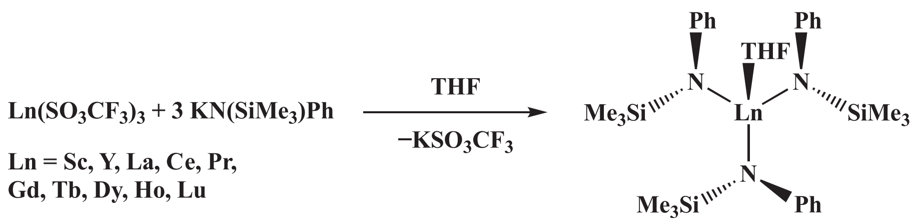

(1)

The complexes exhibited the pale colors typical for the rare-earth metals in their +3 oxidation state. The $^{29}Si\{^{1}H\}$ NMR spectra of **1-Sc**, **1-La** and **1-Lu** exhibit a single resonance, but **1-Y** has two resonances separated by 0.01 ppm. In variable-temperature NMR experiments in THF-d_8, no change was observed in the peak-height ratio between the two peaks when the temperature is varied between 0 °C and 50 °C, but the chemical shifts vary from −10.45 and −10.46 ppm to −10.41 and −10.42 ppm, respectively. The two peaks are only visible on a 600 MHz spectrometer; only one peak is observed in a 500 MHz spectrum.

All of the **1-Ln** complexes crystallize in the $P2_1/n$ space group and have similar structures, Fig. 1. The larger metals are isomorphous with Nd[N(SiMe$_3$)Ph]$_3$(THF) [15], but **1-Sc** and **1-Lu** are different and isomorphous with V[N(SiMe$_3$)Ph]$_3$(THF) [23].

The N(SiMe$_3$)Ph ligands in **1-Ln** are arranged so that all of the phenyl groups are on the same side of the N$_3$ donor atom plane as the coordinated THF. Hence, the THF is bound in a pocket of three phenyl rings in these complexes. The phenyl groups are not symmetry equivalent, but the donor atom arrangement is nearly ideally tetrahedral around each Ln as shown by the structural parameter τ_4' [24] in Table 1. Table 1 also shows the metrical parameters of **1-Ln** vs the more common Ln[N(SiMe$_3$)$_2$]$_3$ [25–30]. In general, the **1-Ln** complexes have longer Ln–N distances which is consistent with the higher formal coordination number [31]. The **1-Ln** complexes also have more variable dihedral angles, compared to Ln[N(SiMe$_3$)$_2$]$_3$, between the N$_3$ plane and the plane defined by the Si-N-C$_{ipso}$ atoms of the ligands in **1-Ln** or by the Si–N–Si plane in Ln[N(SiMe$_3$)$_2$]$_3$. For each metal, the 3.745(1)–4.059(2) Å Ln…C(SiMe$_3$) distances of **1-Ln** are all much longer than those for the analogous Ln[N(SiMe$_3$)$_2$]$_3$ complexes such that no anagostic interactions can be claimed in the **1-Ln** series.

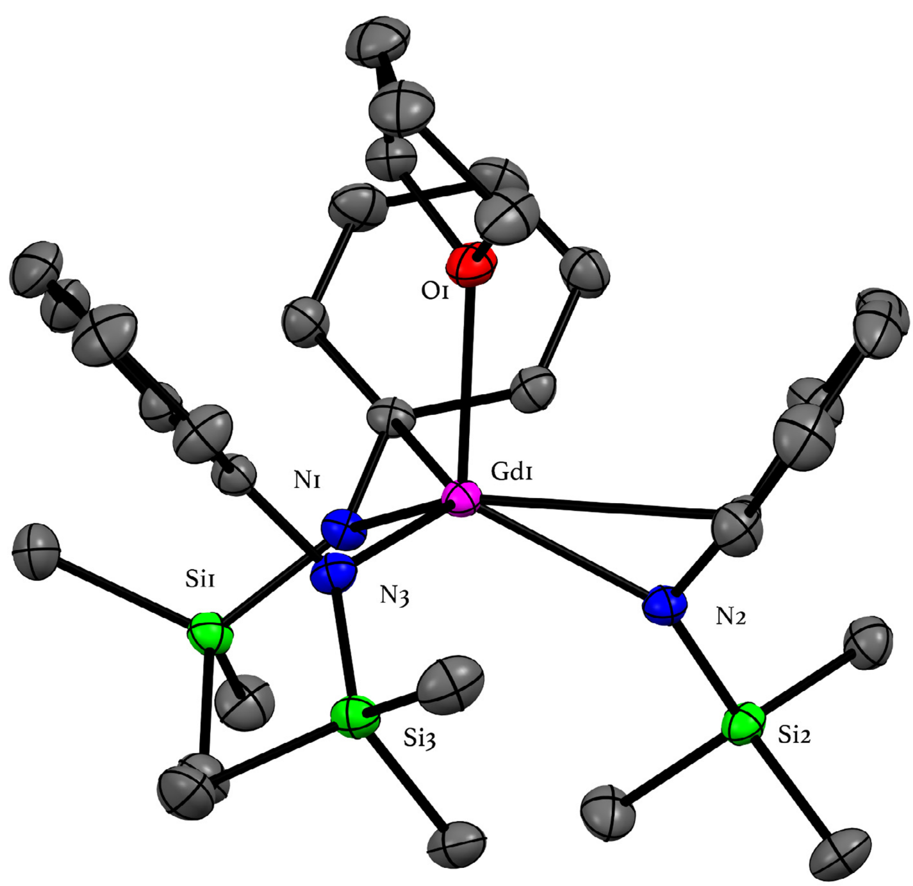

Fig. 1. Thermal ellipsoid plot of Gd[N(SiMe$_3$)Ph]$_3$(THF), **1-Gd**, thermal ellipsoids at the 50% probability level. Hydrogen atoms are omitted for clarity. The structure is representative of all **1-Ln**.

Table 1
Metrical parameters of Ln[N(SiMe$_3$)Ph]$_3$(THF), **1-Ln**, and Ln[N(SiMe$_3$)$_2$]$_3$ complexes with distances in Å, angles in degrees, the Guzei G parameter in % [20], and Θ = dihedral angle between the N$_3$ plane and the Si-N-C$_{ipso}$ or Si–N–Si plane.

Compound	Ln–N range	Average Ln–N	Shortest Ln...C(SiMe$_3$) range	Ln–C$_{ipso}$ range	τ_4'	G	Θ	Ref.
1-La	2.375(1)–2.380(1)	2.377(1)	3.794(1)–4.059(2)	2.879(1)–3.132(1)	0.91	82	49 55 58	This work
1-Ce	2.342(1) –2.351(1)	2.346(2)	3.764(2)–4.041(2)	2.854(2)–3.121(2)	0.90	83	49 55 59	This work
Ce[N(SiMe$_3$)$_2$]$_3$	2.318–2.320	2.319	3.106–3.549	–	–	†	49	[26]
1-Pr	2.315(1)–2.330(2)	2.325(3)	3.782(2)–4.037(2)	2.851(2)–3.097(2)	0.91	83	49 55 58	This work
1-Nd	2.298(2) –2.319(2)	2.308(3)	3.818(4)–4.039(4)	2.846(4)–3.069(4)	0.92	83	48 55 58	[15]
Nd[N(SiMe$_3$)$_2$]$_3$	2.240–2.245	2.243	3.300	–	–	†	50	[29]
1-Gd	2.250(1) –2.274(1)	2.263(2)	3.823(2)–4.020(2)	2.864(2)–3.052(2)	0.92	85	49 55 58	This work
1-Tb	2.239(2) –2.261(2)	2.251(3)	3.769(3) –4.025(3)	2.801(2)–3.068(2)	0.91	85	49 54 58	This work
Tb[N(SiMe$_3$)$_2$]$_3$	2.230	2.230	2.920–3.790	–	–	85	50	[27]
1-Dy	2.219(2) –2.243(2)	2.234(3)	3.764(2)–3.990(2)	2.813(2)–3.054(2)	0.92	86	50 54 57	This work
Dy[N(SiMe$_3$)$_2$]$_3$	2.213–2.215	2.214	2.970–3.724	–	–	85	50	[28]
1-Ho	2.214(2) –2.231(2)	2.225(3)	3.801(2) –3.988(2)	2.811(2)–3.042(2)	0.93	86	49 54 57	This work
1-Y	2.216(1)–2.242(1)	2.230(1)	3.795(2)–3.988(2)	2.816(2)–3.046(2)	0.93	86	50 54 57	This work
Y[N(SiMe$_3$)$_2$]$_3$	2.222–2.224	2.223	2.977–3.736	–	–	†	50	[30]
1-Lu	2.167(2) –2.187(2)	2.180(3)	3.791(3) –3.940(3)	2.825(3)–3.011(3)	0.95	87	49 55 56	This work
Lu[N(SiMe$_3$)$_2$]$_3$	2.190–2.192	2.191	2.887–3.857	–	–	86	49	[25]
1-Sc	2.057(1) –2.085(1)	2.073(1)	3.745(1)–3.878(2)	2.798(1)–2.393(1)	0.94	90	48 55 55	This work
Sc[N(SiMe$_3$)$_2$]$_3$	2.048(2)–2.057(2)	2.052(3)	2.971(3)–3.801(3)	–	–	87	48 49 52	[33]

†G parameter unavailable as crystal structure excludes H atoms.

2.2. Ln[N(SiMe$_3$)Cy]$_3$(THF) complexes

Reactions of Ln(OTf)$_3$ (Ln = Y, Ho) with LiN(SiMe$_3$)Cy were examined for comparison with **1-Ln**. The complexes Y[N(SiMe$_3$)Cy]$_3$(THF), **2-Y**, and Ho[N(SiMe$_3$)Cy]$_3$(THF), **2-Ho**, were similarly generated according to Eq. (2), but they proved to be more challenging to purify and crystallize than **1-Ln**. The X-ray crystal structures, Fig. 2, are included here to report the existence of these compounds. The ^{1}H and ^{13}C{^{1}H} NMR spectra of **2-Y** are similar to those of **1-Y**. In C$_6$D$_6$, the Me$_3$Si ^{1}H resonance of **2-Y** is at 0.40 ppm, compared to 0.47 ppm in **1-Y**. The ^{29}Si{^{1}H} NMR of **2-Y** has two closely-spaced resonances as found for **1-Y**.

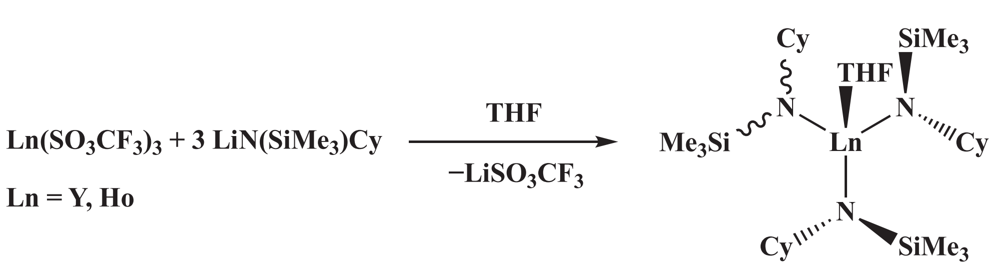

(2)

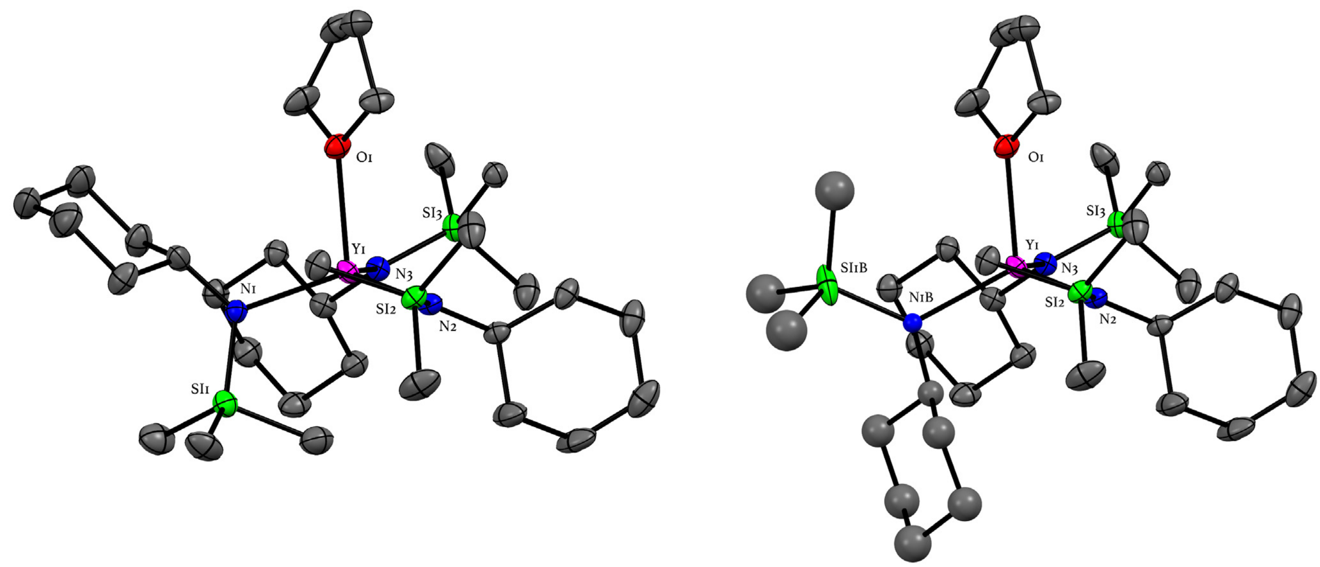

Fig. 2. Thermal ellipsoid plots, thermal ellipsoids drawn at the 50% probability level, of the two disordered structures of **2-Y** which are representative of **2-Ln**. The minor component was refined isotropically. Hydrogen atoms are omitted for clarity. The left plot is the 81% occupancy structure and the right plot is the 19% occupancy structure.

Table 2
Comparison of metrical parameters of Ln[N(SiMe$_3$)Cy]$_3$(THF), **2-Ln**, with Ln[N(SiMe$_3$)Ph]$_3$(THF), **1-Ln**, for Ln = Y, Ho along with Y[N(SiMe$_3$)$_2$]$_3$ with distances in Å, angles in degrees, the Guzei G parameter in % [19], and Θ = dihedral angle between the N$_3$ plane and the Si-N-C$_{ipso}$ or Si–N–Si plane. Multiple sets of Θ, G, and τ_4' values occur when one ligand is disordered over 2 positions.

Complex	Ln–N range	Average Ln-N	Shortest Ln. . .C(SiMe$_3$) range	Ln–C$_{ipso}$ range	τ_4'	G	Θ		Ref.
1-Y	2.216(1)–2.242(1)	2.230(1)	3.795(2)–3.988(2)	2.816(2)–3.046(2)	0.93	86	50 54 57		This work
2-Y	2.217(2)–2.27(2)	2.23(2)	3.169(3)–3.87(2)	2.93(1)–3.177(3)	0.87 0.88	85 83	29 31 80	25 38 87	This work
Y[N(SiMe$_3$)$_2$]$_3$	2.222–2.224	2.223	2.977–3.736	–	–	†	50		[30]
1-Ho	2.214(2) –2.231(2)	2.225(3)	3.801(2)–3.988(2)	2.811(2)–3.042(2)	0.93	86	49 54 57		This work
2-Ho	2.204(6)–2.23(2)	2.22(2)	3.210(6)–3.85(4)	2.98(3)–3.143(6)	0.88 0.88	85 83	30 31 73	26 38 83	This work

†G parameter unavailable as crystal structure excludes H atoms.

X-ray crystallography revealed that complexes **2-Y** and **2-Ho** both crystallize in $P2_1/n$ and are isomorphous. Metrical parameters of **2-Ln** are compared to **1-Ln** and Ln[N(SiMe$_3$)$_2$]$_3$ in Table 2. In contrast to **1-Ln**, the three ligands in **2-Ln** are not ordered in a regular fashion with respect to the N$_3$ plane and the THF ligand. In **2-Ln**, two ligands are oriented with the SiMe$_3$ groups on the side of the bound THF, but the third N(SiMe$_3$)Cy ligand is disordered over two positions, as indicated by the wavy lines in Eq. (2). This third ligand has the SiMe$_3$ groups oriented on the same side as the other two with 19% and 21% occupancy for **2-Y** and **2-Ho**, respectively, and with the complementary occupancies, 81% and 79%, respectively, on the other side.

2.3. Degree of steric saturation

The steric saturation effected by the ligands in **1-Ln** and **2-Ln** was compared to that of Ln[N(SiMe$_3$)$_2$]$_3$ and select other rare earth amide complexes using the solid angle G parameter of Guzei [20], previously used to measure the amount of steric saturation in lanthanide amides and main group amides [22,32]. This method provides an estimation of the percentage of the coordination sphere of the metal that is protected by the ligands. A G parameter of 100% indicates that the ligands completely shield the metal from exogenous substrates, while a G parameter of 50% means that the ligands cover only half the coordination sphere of the metal. In Fig. 3, G parameters of Ln[N(SiMe$_3$)$_2$]$_3$ complexes were plotted alongside those of **1-Ln** and **2-Ln** for comparison [25,27,33–36]. The G parameters are plotted against the six-coordinate ionic radius [31] of the metal contained in the complex. Two G values are given for each **2-Ln** complex because the different orientations of the disordered ligand provide different amounts of steric saturation. As might be expected, the G parameter is proportional to the ionic radius [31] of the Ln in these complexes and varies smoothly across the Ln series. The G parameters of the unsolvated hypothetical species, “Ln[N(SiMe$_3$)Ph]$_3$” and “Ln[N(SiMe$_3$)Cy]$_3$” were also calculated. These calculations gave G parameters from 69-74%, well outside of the range found for the isolable complexes **1-Ln** (82–90%), **2-Ln** (83–85%), Ln[N(SiMe$_3$)$_2$]$_3$ (84–87%), La[N(SiMe$_3$)(SiMe$_2{}^t$Bu)]$_3$

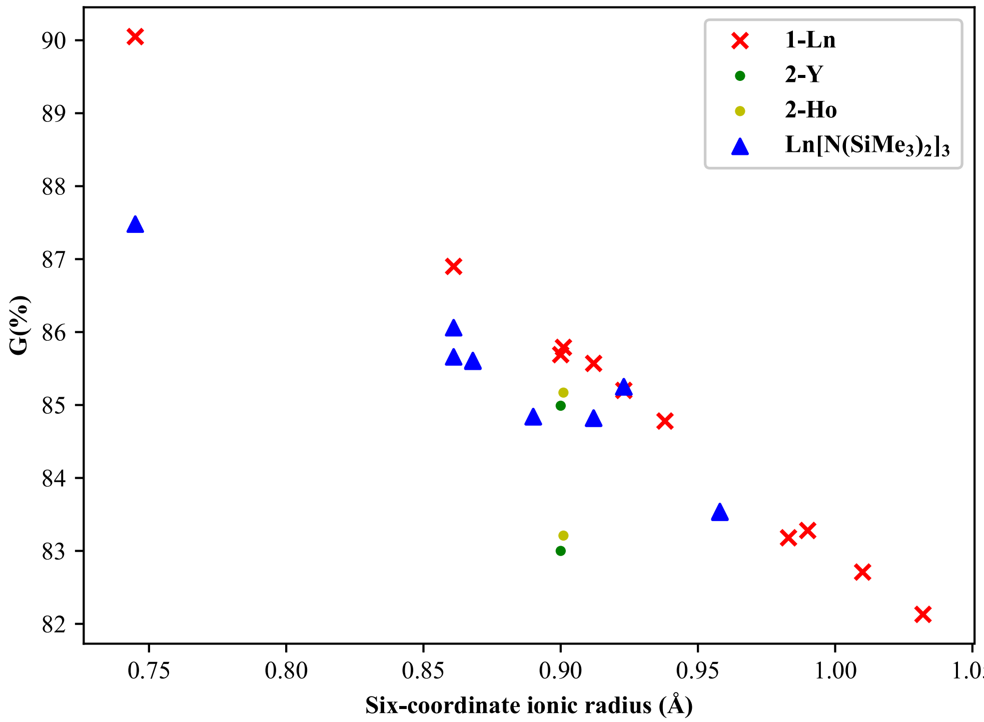

Fig. 3. Plot of the G parameters of **1-Ln**, **2-Ln**, and $Ln[N(SiMe_3)_2]_3$ vs the six-coordinate ionic radius [31] of the corresponding Ln(III) ion. Two points are included for each **2-Ln** and some $Ln[N(SiMe_3)_2]_3$ when the data were modeled with two disordered structures, which have different G parameters.

(87%), $Ce[N(SiMe_3)(SiMe_2{}^tBu)]_3$ (88%), and $La[N(SiMe_2{}^tBu)_2]_3$ (92%) [22].

3. Discussion

The syntheses of $Ln[N(SiMe_3)Ph]_3(THF)$, **1-Ln**, can be accomplished from $Ln(OTf)_3$ and $KN(SiMe_3)Ph$ as well as the previously-known route from $LnCl_3$ and $LiN(SiMe_3)Ph$ [15]. The ease of preparing anhydrous $Ln(OTf)_3$ compared to $LnCl_3$ may make triflates an attractive starting material for other types of lanthanide complexes. The crystal structures of **1-Ln** show that these complexes crystallize with one molecule of THF in contrast to the unsolvated $Ln[N(SiMe_3)_2]_3$ series [25,27,33–36]. Analysis of the degree of steric saturation using the Guzei G parameter indicates why the mono-solvates are isolated. Without THF, the $Ln[N(SiMe_3)Ph]_3$ and $Ln[N(SiMe_3)Cy]_3$ complexes would not have G parameters in the range found for the isolable complexes. Hence, both $N(SiMe_3)Ph$ and $N(SiMe_3)Cy$ occupy less space around the rare-earth ion than $N(SiMe_3)_2$.

The G parameter also shows that $N(SiMe_3)Cy$ with all three cyclohexyl groups on one side of the N_3 plane protects a smaller area of the metal than the other orientation of ligands in **2-Ln**. This lower degree of steric saturation may enhance reactivity and provide a channel for decomposition. This could be an Achilles heel that contributes to the difficulty of synthesizing these complexes. This disorder could also contribute to problems in crystallizing these complexes, since there is not one optimum geometry.

4. Conclusion

The $N(SiMe_3)Ph$ and $N(SiMe_3)Cy$ amide ligands form crystallographically characterizable complexes of the rare-earth metals like the more common $N(SiMe_3)_2$ ligands, but they are isolated as THF solvates to achieve steric saturation. $Ln[N(SiMe_3)Ph]_3(THF)$ complexes are available with both large and small metals ranging from La to Sc, but the $Ln[N(SiMe_3)Cy]_3(THF)$ complexes were isolated only for the similarly-sized Ho and Y. Salt metatheses starting with $Ln(OTf)_3$ demonstrated that triflates are viable alternatives to chloride precursors in these syntheses.

5. Experimental details

All manipulations and syntheses described below were conducted with the rigorous exclusion of air and water using standard Schlenk line and glovebox techniques under an argon atmosphere. Solvents were sparged with UHP argon and dried by passage through columns containing Q-5 and molecular sieves prior to use. Deuterated NMR solvents were dried over NaK alloy, degassed by three freeze–pump-thaw cycles, and vacuum transferred before use. ^1H, $^{13}C\{^1H\}$, and $^{29}Si\{^1H\}$ (using the INEPT pulse sequence) NMR spectra were recorded on Bruker AVANCE600, CRYO500, or GN500 spectrometers ($^{13}C\{^1H\}$ NMR spectra on the CRYO500 spectrometer operating at 125 MHz, $^{13}C\{^1H\}$ NMR spectra on the AVANCE600 operating at 151 MHz, $^{29}Si\{^1H\}$ at 119 MHz on the AVANCE600, ^{89}Y at 24 MHz on the GN500) at 298 K unless otherwise stated and referenced internally to residual protio-solvent resonances, to external $SiMe_4$ for $^{29}Si\{^1H\}$ experiments, or to external $Y(NO_3)_3$ for $^1H–^{89}Y$ experiments. NMR resonances were assigned with the help of HMQC and HSQC experiments. Elemental analyses were conducted on a Perkin-Elmer 2400 Series II CHNS elemental analyzer. The $Ln(OTf)_3$ precursors (Strem) were dried at 220 °C at 10^{-5} Torr for 2 days before use [37], except for $Ce(OTf)_3$. The cerium triflate was dried at 220 °C at 10^{-5} Torr for 2 days, then pulverized and dried again at 220 °C at 10^{-5} Torr for 2 more days. $KN(SiMe_3)Ph$ [38] and $LiN(SiMe_3)Cy$ [19] were synthesized using published preparations.

5.1. $Ln[N(SiMe_3)Ph]_3(THF)$, **1-Ln**

$Ln(OTf)_3$ (1 equiv) and $KN(SiMe_3)Ph$ (3 equiv) were suspended together in THF and stirred overnight. The solvent was removed from the suspension *in vacuo* and the solids were extracted with toluene (10–15 mL in three portions). Solvent was removed from the solution *in vacuo* and the crude solids were recrystallized in procedures detailed for each of the **1-Ln** compounds. Each complex was purified by trituration with pentane; this was done at low temperature to minimize the solubility of the complex.

5.1.1. 1-Sc

The solids were chilled to −15 °C to form a rubbery puck of crude orange solids, which was triturated with −30 °C pentane (15 × 1 mL) to form a free-flowing powder. The solids were dried *in vacuo* to give beige $Sc[N(SiMe_3)Ph]_3(THF)$, **1-Sc** (350 mg, 29% yield). Colorless X-ray quality crystals were grown overnight from a pentane solution at −30 °C. ^1H NMR (THF-d_8): δ 7.15 (t, *J* = 7.7 Hz, 6H, *m*-H), 6.95 (d, *J* = 7.7 Hz, 6H, *o*-H), 6.85 (t, *J* = 7.3 Hz, 3H, *p*-H), 3.61 (m, 6H, 2,5-THF-CH_2), 1.77 (m, 6H, 3,4-THF-CH_2), 0.11 ppm (s, 27H, SiMe_3). $^{13}C\{^1H\}$ NMR (THF-d_8): δ 152.8 (*i*-C), 129.5 (*m*-C), 128.4 (*o*-C), 122.0 (*p*-C), 68.2 (2,5-THF-CH_2), 26.4 (3,4-THF-CH_2), 2.2 (SiMe_3). $^{29}Si\{^1H\}$ NMR (THF-d_8, ppm): δ −6.02. IR (cm^{-1}): 3075w, 3047w, 2959w, 2892w, 1588m, 1565w, 1499w, 1476w, 1352m sh, 1330m, 1272m sh, 1243s, 1231s, 1217s, 1206s, 1189s sh, 1168m, 1078w, 1031s, 1003m, 933m, 912m, 901m, 884m, 848m, 831s br, 797s, 754m, 738m, 733m, 702m, 683m, 669m, 634s, 624s. *Anal. Calc.* for $Sc[N(SiMe_3)Ph]_3(THF)$ $C_{27}H_{42}N_3ScSi_3O$: C, 61.04; H, 8.26; N, 6.89. Found: C, 44.60; H, 6.19; N, 4.55%. Incomplete combustion was observed with this sample as sometimes is the case with rare-earth complexes [22,39–42], but the observed CHN ratio, $C_{31}H_{31}N_3$, is close to the calculated.

5.1.2. 1-Y

The crude yellow solids were chilled to −30 °C and triturated with −30 °C pentane (2 × 1 mL). Decanting the solvent and removal of the residual solvent *in vacuo* gave beige solids, $Y[N(SiMe_3)Ph]_3(THF)$, **1-Y** (260 mg, 41% yield). Colorless X-ray quality crystals were grown from a saturated pentane solution at −30 °C overnight. ^1H NMR (C_6D_6): δ 7.14 (d, *J* = 7.6 Hz, 6H, *o*-H), 6.96 (t, *J* = 7.8 Hz, 6H, *m*-H), 6.53 (t, *J* = 7.2 Hz, 3H, *p*-H), 0.37 ppm (s, 27H, SiMe_3). $^{13}C\{^1H\}$ NMR (C_6D_6): δ 156.4 (*i*-C), 129.4 (*m*-C), 125.5 (*o*-C), 117.9 (*p*-C), 2.9 (SiMe_3) ppm. $^{29}Si\{^1H\}$ NMR (C_6D_6): δ −7.06, −7.07 ppm. ^{89}Y NMR (C_6D_6): δ 587 ppm. Lack of THF resonances in the ^1H and $^{13}C\{^1H\}$ spectra indicate desolvation may have occurred. Direct observation of the ^{89}Y nucleus was unsuccessful, but the signal could be observed in 2D ^1H–^{89}Y gHMBC experiments. IR (cm^{-1}): 3691w, 3068w, 3051w, 3027w, 2950m, 2895m, 2865w sh, 1584m, 1561w, 1534w br, 1489m, 1474m, 1458w, 1441w, 1396w br, 1351m, 1329w, 1299w, 1283w, 1261m sh, 1250m sh, 1238s, 1219s, 1181m, 1168m, 1153m, 1106m, 1081w, 1068w, 1041w, 1027w, 1008w, 992m, 973w, 960w, 937s, 910s, 895m, 885m, 836m sh, 824s, 802w, 788m, 752m, 740m, 726m sh, 707s, 681 m, 671 m, 643w, 626 m, 614 m. *Anal. Calc.* for $Y[N(SiMe_3)Ph]_3$ $C_{27}H_{42}N_3Si_3Y$: C, 55.74; H, 7.28; N, 7.22. Found: C, 53.28; H, 7.20; N, 5.91%. Incomplete combustion was observed with this sample as sometimes is the case with rare-earth complexes [22,39–42], but the observed CHN ratio, $C_{27}H_{43}N_3$, is close to the calculated and consistent with the loss of 1 equiv of THF as seen in the ^1H NMR.

5.1.3. 1-La

The brown-yellow solids were washed with −30 °C pentane (3 × 1 mL), then recrystallized from 2 mL of 1:1 pentane:toluene to give colorless crystals of $La[N(SiMe_3)Ph]_3(THF)$, **1-La** (50 mg, 15%). X-ray quality crystals were grown from 1:1 pentane:toluene at −30 °C in 3 hours. ^1H NMR (C_6D_6): δ 7.03 (d, *J* = 7.4 Hz, 6H, *o-H*), 6.98 (t, *J* = 7.6 Hz, 6H, *m*-H), 6.50 (t, *J* = 6.99 Hz, 3H, *p*-H), 3.52 (m, 3H, 2,5-THF-CH_2), 1.40 (m, 4H, 3,4-THF-CH_2), 0.37 ppm (s, 27H, SiMe_3). $^{13}C\{^1H\}$ NMR (C_6D_6): δ 155.9 (*i*-C), 130.4 (*m*-C), 123.6 (*o*-C), 117.4 (*p*-C), 67.8 (2,5-THF-CH_2), 25.8 (3,4-THF-CH_2), 2.5 ppm (SiMe_3). $^{29}Si\{^1H\}$ NMR (C_6D_6). δ −8.80 ppm. IR (cm^{-1}): 3737w, 3637w, 3066w, 3047w, 2964m, 2948m, 2891m, 2880m, 2530w, 1583m, 1558w, 14788m sh, 1475s, 1397w br, 1351m, 1355w, 1296w, 1250m sh, 1239s, 1226m sh, 1183m, 1176m, 1150w, 1108m, 1076w, 1047m, 1029w, 991m, 962w, 902m, 884m, 827s, 780m, 749m, 727w, 703m, 698m, 685w, 673w, 627m, 622m. *Anal. Calc.* for $C_{31}H_{50}LaN_3OSi_3$: C, 52.89; H, 7.16; N, 5.97. Found: C, 43.86; H, 5.79; N, 4.90%. Incomplete combustion was observed with this sample as noted above [22,39–42], but the observed CHN ratio, $C_{31}H_{49}N_3$, is close to the calculated.

5.1.4. 1-Ce

The yellow solids were triturated with −30 °C pentane (4 mL in portions) and dried *in vacuo* to give gold $Ce[N(SiMe_3)Ph]_3(THF)$, **1-Ce** (340 mg, 49% yield). X-ray quality crystals were grown from 1:1 hexane:toluene at −30 °C overnight. ^1H NMR (C_6D_6): δ 13.69 (s, 6H, *o-H*), 5.61 (d, *J* = 4.7 Hz, 6H, *m*-H), 4.28 (s, 3H, *p*-H), 0.33 (s, 27H, SiMe_3) −2.04 (br, $\nu_{1/2}$ = 143 Hz, 6H, 3,4-THF-CH_2), −5.36 ppm (br, $\nu_{1/2}$ = 613 Hz, 5H, 3,4-THF-CH_2). IR (cm^{-1}): 3063w, 3023w, 2946 m, 2894w, 1582s, 1558w, 1487m, 1472s, 1439w, 1396w, 1374w, 1325w, 1295w, 1254sh, 1234br, 1176m, 1167m, 1152w, 1075w, 1066w, 1025sh, 1016m, 992m, 936m, 912s, 896m, 883m, 835sh, 820s br, 798w, 779s, 751m, 738m, 729sh, 718w, 698s, 680m, 669m. *Anal. Calc.* for $C_{31}H_{50}CeN_3OSi_3$: C, 52.80; H, 7.15; N, 5.96. Found: C, 47.20; H, 6.15; N, 4.90%. Incomplete combustion was observed with this sample as noted above [22,39–42], but the observed CHN ratio, $C_{31}H_{48}N_3$, is close to the calculated.

5.1.5. 1-Pr

The orange solids were triturated with −30 °C pentane (3 × 1 mL) and dried *in vacuo* to give green-yellow crystals, $Pr[N(SiMe_3)Ph]_3(THF)$, **1-Pr** (140 mg, 20% yield). X-ray quality crystals were grown overnight from a pentane solution at −30 °C. IR (cm^{-1}): 3636w, 3067w, 3048w, 2965w, 2949m, 2891m, 2880w sh, 1584s, 1560w, 1489m sh, 1475s, 1397w br, 1351m, 1335w, 1299w sh, 1281w sh, 1250m sh, 1239s, 1221s, 1183m, 1177m, 1152w, 1108m, 1076m, 1052m, 1047m, 1028w, 992m, 962w, 912m sh, 901s, 884m, 826s, 781s, 750s, 718m, 702s, 673m, 625m. *Anal. Calc.* for $C_{31}H_{50}N_3OPrSi_3$: C, 52.74; H, 7.14; N, 5.95. Found: C, 49.31; H, 6.73; N, 5.48%. Incomplete combustion was observed with this sample as noted above [22,39–42], but the observed CHN ratio, $C_{31}H_{50}N_3$, matches to the calculated.

5.1.6. 1-Gd

The orange solids were triturated with −30 °C pentane (3 × 1 mL), then dissolved in 2:6:1 pentane:toluene:THF (∼5 mL) and left at −30 °C overnight. The resulting colorless crystals were washed with −30 °C pentane and dried *in vacuo* to give white crystals, $Gd[N(SiMe_3)Ph]_3(THF)$, **1-Gd** (210 mg, 29% yield). X-ray quality crystals were grown overnight from a concentrated toluene solution at −30 °C. IR (cm^{-1}): 3646w, 3066w, 6048w 2960m, 2947m, 2893m, 2879m, 1584m, 1581m, 1574w sh, 1560w, 1552w, 1488m sh, 1475m, 1399w br, 1351m, 1355w, 1300w sh, 1280w, 1255m sh, 1250m sh. 1239s, 1225m, 1219m, 1183m, 1176m, 1150w, 1108m, 1080w, 1076w, 1052m, 1047m, 1028w, 992m, 962w, 920w sh, 910m sh, 901s, 883s, 827s, 781s, 749s, 727m, 703s, 698sm 685w, 673m, 642w, 626m, 611m. *Anal. Calc.* for $C_{31}H_{50}GdN_3OSi_3$: C, 51.55; H, 6.98; N, 5.82. Found: C, 49.54; H, 6.36; N, 5.33%. Incomplete combustion was observed with this sample as noted above [22,39–42], but the observed CHN ratio, $C_{31}H_{47}N_3$, is close to the calculated.

5.1.7. 1-Dy

The grey-purple solids were triturated with pentane (3 × 1 mL) and the resulting solids were dissolved in 2:6:1 pentane:toleuene:

THF (~5 mL), then left at −30 °C overnight. The solution was then concentrated to ~2 mL and pentane was added. The solution was left at −30 °C for three days and crystals resulted, which were washed with −30 °C pentane (3 × 1 mL) and dried *in vacuo* to give white–grey crystals, $Dy[N(SiMe_3)Ph]_3(THF)$, **1-Dy** (100 mg, 14% yield). X-ray quality crystals were grown overnight from a concentrated toluene solution at −30 °C. IR (cm^{-1}): 3067w, 3039w, 2959m, 2948m, 2891m, 2879m, 1580m, 1572 m sh, 1560w, 1552w, 1489m, 1475s, 1398w br, 1367w, 1351w, 1335w, 1296w sh, 1284w sh, 1251m, 1239s, 1225m, 1220m, 1183m, 1176m, 1053m, 1047m, 1028m, 992m, 962w, 922w sh, 812m sh, 901s, 883s, 827s, 787s, 781s, 748m, 702m, 699m, 685m, 673s, 626m, 609w. *Anal. Calc.* for $Dy[N(SiMe_3)Ph]_3$, a loss of 1 molecule of THF; $C_{27}H_{42}DyN_3Si_3$: C, 49.48; H, 6.46; N, 6.41. Found: C, 45.23; H, 5.78; N, 5.62%. Incomplete combustion was observed with this sample as noted above [22,39–42], but the observed CHN ratio, $C_{27}H_{41}N_3$, is close to the calculated.

5.1.8. 1-Ho

X-ray quality crystals were grown overnight from a 1:2 pentane:toluene solution at −30 °C to give pink $Ho[N(SiMe_3)Ph]_3(THF)$, **1-Ho** (160 mg, 44% crystalline yield). *Anal. Calc.* for $C_{31}H_{50}HoN_3OSi_3$: C, 51.01; H, 6.90; N, 5.76. Found: C, 46.10; H, 6.75; N, 5.19%. Incomplete combustion was observed with this sample as noted above [22,39–42], but the observed CHN ratio, $C_{31}H_{54}N_3$, is close to the calculated.

5.1.9. 1-Tb

X-ray crystals were grown overnight from a 1:6 pentane:-toluene solution at −30 °C, then washed with −30 °C pentane (1 × 3 mL) to yield pale yellow-green $Tb[N(SiMe_3)Ph]_3(THF)$, **1-Tb** (300 mg, 52% yield). *Anal. Calc.* for $C_{31}H_{50}N_3OSi_3Tb$: C, 51.43; H, 6.96; N, 5.80. Found: C, 50.0; H, 6.88; N, 5.66%. Incomplete combustion was observed with this sample as noted above [22,39–42], but the observed CHN ratio, $C_{31}H_{51}N_3$, is close to the calculated.

5.1.0. 1-Lu

The light-brown solids were washed with pentane (3 × 1 mL) then dissolved in 2:6:1 pentane:toluene:THF (5 mL) and left at −30 °C. Small, colorless crystals precipitated, which were washed with −30 °C pentane (3 × 1 mL) and dried *in vacuo* to give $Lu[N(SiMe_3)Ph]_3(THF)$, **1-Lu** (90 mg, 25% yield). X-ray quality crystals were grown overnight by recrystallizing the solids first from a solution made in pentane and toluene, then crystallizing the resulting material from a solution in a mixture of pentane, toluene, and THF at −30 °C. ^1H NMR (C_6D_6): δ 7.20 (d, *J* = 7.5 Hz, 6H, *o*-H), 7.12 (t, *J* = 7.8 Hz, 6H, *m*-H), 6.78 (t, *J* = 7.3 Hz, 3H, *p*-H), 0.46 ppm (s, 27H, Si*Me*$_3$). $^{13}C\{^1H\}$ NMR (C_6D_6): δ 152.9 (*i*-C), 129.9 (*m*-C), 126.4 (*o*-C), 120.6 (*p*-C), 2.4 ppm (Si*Me*$_3$). $^{29}Si\{^1H\}$ NMR (C_6D_6): δ −5.52 ppm. IR (cm^{-1}): 3636w, 3067w, 3047w, 3024w, 2966m, 2949m, 2893m, 2877m, 1584m, 1572m sh, 1560w, 1553w, 1489m sh, 1475s, 1458m sh, 1395w br, 1351w, 1334w, 1299w sh, 1281w sh, 1250m sh, 1239s, 1226s, 1219m sh, 1183m, 1177m, 1154w, 1150w, 1108m, 1080w, 1076w, 1053m, 1047m, 1029m, 992m, 962w, 923w sh, 911m sh, 901s, 883s 827s, 786m, 782m, 749s, 723m, 703s, 699s, 685m, 674m, 626m, 609w. Lack of THF resonances in the ^1H and $^{13}C\{^1H\}$ spectra indicate desolvation may have occurred. *Anal. Calc.* for $C_{31}H_{50}LuN_3OSi_3$: C, 50.32; H, 6.81; N, 5.68. Found: C, 49.07; H, 6.64; N, 5.46%. Incomplete combustion was observed with this sample as noted above [22,39–42], but the observed CHN ratio, $C_{31}H_{50}N_3$, matches the calculated.

*5.2. $Y[N(SiMe_3)Cy]_3(THF)$, **2-Y***

$LiN(SiMe_3)Cy$ (0.20 g, 1.1 mmol) dissolved in THF (5 mL) was added to solid $Y(OTf)_3$ (0.20 g, 0.37 mmol). After stirring overnight, a hazy yellow solution was present. Solvent was removed *in vacuo* to give yellow-white oily solids, which were extracted with toluene (10 mL) in three portions. The resulting yellow suspension was centrifuged and the supernatant was filtered away from white solids to give a yellow solution. Solvent was removed *in vacuo* to give an orange oil, which was suspended in 1 mL toluene and left at −30 °C overnight to precipitate any entrained insoluble material. White solids were removed by filtration and the solvent was stripped from the supernatant to give orange $Y[N(SiMe_3)Cy]_3(THF)$, **2-Y** (175 mg, 70% yield). X-ray quality colorless crystals were grown from a solution made from 0.5 mL hexane and minimum toluene left at −30 °C for six days. ^1H NMR (C_6D_6): δ 3.83 (s, 5H, 3,5-THF-C*H*$_2$), 3.07 (m, 3H, 1-Cy-C*H*), 2.06 (d, *J* = 12.0 Hz, 6H, 2,6-Cy-C*H*$_2$), 1.84 (d, *J* = 12.2 Hz, 6H, 3,5-Cy-C*H*$_2$), 1.65 (d, *J* = 12.1 Hz, 3H, 4-Cy-C*H*$_2$), 1.59 (q, *J* = 12.1 Hz, 6H, 2,6-Cy-C*H*$_2$), 1.40 (q, *J* = 12.5 Hz, 6H, 3,5-Cy-C*H*$_2$), 1.25 (s, 5H, 3,4-THF-C*H*$_2$), 1.18 (q, *J* = 11.8 Hz, 3H, 4-Cy-C*H*$_2$), 0.40 ppm (s, 27H, Si*Me*$_3$). $^{13}C\{^1H\}$ NMR (C_6D_6): δ 71.8 (2,5-THF-CH_2), 57.4 (1-Cy), 41.1 (2,6-Cy), 27.4 (3,5-Cy), 26.4 (4-Cy), 25.2 (3,4-THF-C*H*$_2$), 4.8 ppm (Si*Me*$_3$). $^{29}Si\{^1H\}$ NMR (C_6D_6): δ −12.47, −12.48 ppm. IR (cm^{-1}): 3733w, 3707w, 3632w, 3595w, 2992m sh, 2981m, 2925s, 2898sh, 2851m, 2666w, 2360w, 2342m, 2329m, 1461w, 1448w, 1325m, 1300m, 1273m sh, 1261s, 1236s, 1194m, 1178m, 1145m, 1116m sh, 1105m, 1066m sh, 1042s, 1018m sh, 986m, 916w, 893m, 872w sh, 853m, 840m, 822s, 798m, 762m, 744m, 728w, 676w sh, 668w, 661w, 635s, 620m.

*5.3. $Ho[N(SiMe_3)Cy]_3(THF)$, **2-Ho***

$LiN(SiMe_3)Cy$ (870 mg, 4.9 mmol) was dissolved in THF (15 mL) and added to a suspension of $Ho(OTf)_3$ (1.02 g, 1.66 mmol) in THF (5 mL) to form a pink suspension. After stirring overnight, a hazy pink-brown solution resulted. Solvent was removed *in vacuo* to give brown solids. The solids were extracted with toluene (20 mL) in three portions. Each portion was centrifuged and the supernatant was filtered, reserving the pink supernatant. Solvent was removed *in vacuo* to give pink solids, which were redissolved in toluene (5 mL), centrifuged, and filtered to remove insoluble. The solution was concentrated to 2 mL and left at −30 °C overnight. The resulting pink solids were washed with −30 °C pentane (3 × 1 mL) and dried *in vacuo* to give pink $Ho[N(SiMe_3)Cy]_3(THF)$, **2-Ho** (190 mg, 15%). Pink X-ray quality crystals could be grown from a methylcyclohexane solution at −30 °C over two days. IR (cm^{-1}): 3726w, 3631w, 2997w sh, 2982w, 2951m sh, 2924s, 2898m sh, 2847m, 2362w, 2344w, 2324w, 1461w, 1447m, 1386w br, 1342w, 1327w, 1254m, 1236s, 1179w, 1144w, 1103s, 1068m, 1041w, 1013m, 985m, 917w, 906w, 893m, 851s, 840m, 819s, 798m, 760m, 745m, 724m, 694w, 673w, 662m, 636m. *Anal. Calc.* for $Ho[N(SiMe_3)Cy]_3$: $C_{27}H_{60}HoN_3Si_3$: C, 47.97; H, 8.95; N, 6.22. Found: C, 44.32; H, 8.84; N, 4.86%. Incomplete combustion was observed with this sample as noted above [22,39–42], but the observed CHN ratio, $C_{27}H_{64}N_3$, is close to the calculated.

Declaration of interest

The authors declare no conflict of interest.

Acknowledgements

We thank the U.S. National Science Foundation for support of this research under CHE-1565776, Dr. Michael Wojnar and Austin

Ryan for their assistance with X-ray crystallography, Valentine Bratoff for his assistance with matplotlib for preparing figures, and Carter Jones for his CJHUNT (Carter Jones' Highly Useful Numbering Tool) program, which assists in processing crystallography data for use with Solid-G.

Appendix A. Supplementary data

CCDC 1858316–1858327 contains the supplementary crystallographic data for **1-Sc**, **1-Y**, **1-La**, **1-Pr**, **1-Ce**, **1-Gd**, **1-Tb**, **1-Dy**, **1-Ho**, **1-Lu**, **2-Y**, and **2-Ho**. These data can be obtained free of charge via http://www.ccdc.cam.ac.uk/conts/retrieving.html, or from the Cambridge Crystallographic Data Centre, 12 Union Road, Cambridge CB2 1EZ, UK; fax: (+44) 1223-336-033; or e-mail: deposit@ccdc.cam.ac.uk. Supplementary data to this article can be found online at https://doi.org/10.1016/j.poly.2019.04.026.

References

[1] M.F. Lappert, A.V. Protchenko, P.P. Power, A. Seeber, Metal Amide Chemistry, John Wiley & Sons Ltd, Chippenham, 2008.
[2] R. Anwander, Lanthanide amides, in: Organolanthoid Chem. Synth. Struct. Catal., Springer Berlin Heidelberg, Berlin, Heidelberg, 1996, pp. 33–112.
[3] C.A.P. Goodwin, D.P. Mills, Silylamides: towards a half-century of stabilising remarkable f-element chemistry, Organomet. Chem. 41 (2017) 123.
[4] D. Schneider, T. Spallek, C. Maichle-Mössmer, K.W. Törnroos, R. Anwander, Cerium tetrakis(diisopropylamide)-a useful precursor for cerium(IV) chemistry, Chem. Commun. 50 (2014) 14763.
[5] W.J. Evans, R. Anwander, J.W. Ziller, S.I. Khan, Heteropolyagostic interactions in lanthanide(III) diisopropylamido complexes, Inorg. Chem. 34 (1995) 5927.
[6] T. Spallek, O. Heß, M. Meermann-Zimmermann, C. Meermann, M.G. Klimpel, F. Estler, D. Schneider, W. Scherer, M. Tafipolsky, K.W. Törnroos, C. Maichle-Mössmer, P. Sirsch, R. Anwander, Synthesis and structural diversity of trivalent rare-earth metal diisopropylamide complexes, Dalton Trans. 45 (2016) 13750.
[7] H.C. Aspinall, M.R. Tillotson, Four-coordinate lanthanide di-isopropylamides: $[Li(THF)Ln(N^{i}Pr_2)_4]$ (Ln = La, Y, Yb), Polyhedron 13 (1994) 3229.
[8] W.J. Evans, R. Anwander, R.J. Doedens, J.W. Ziller, The use of heterometallic bridging moieties to generate tractable lanthanide complexes of small ligands, Angew. Chem., Int. Ed. 33 (1994) 1641.
[9] E.C. Alyea, D.C. Bradley, R.G. Copperthwaite, Three-co-ordinated transition metal compounds. Part I. The preparation and characterization of tris (bistrimethylsilylamido)-derivatives of scandium, titanium, vanadium, chromium, and iron, J. Chem. Soc., Dalton Trans. (1973).
[10] D.C. Bradley, J.S. Ghotra, F.A. Hart, Three-co-ordination in lanthanide chemistry: tris[bis(trimethylsilyl)amido]lanthanide(III) compounds, J. Chem Soc., Chem. Comm. (1972) 349.
[11] D.C. Bradley, J.S. Ghotra, F.A. Hart, Low co-ordination numbers in lanthanide and actinide compounds. Part 1. The preparation and characterization of tris {bis(trimethylsilyl)-amido)lanthanides, J. Chem. Soc., Dalton Trans. (1972) 1021.
[12] R. Anwander, O. Runte, J. Eppinger, G. Gerstberger, E. Herdtweck, M. Spiegler, Synthesis and structural characterisation of rare-earth bis(dimethylsilyl) amides and their surface organometallic chemistry on mesoporous MCM-41, J. Chem. Soc., Dalton Trans. (1998) 847.
[13] A.M. Bienfait, C. Schädle, C. Maichle-Mössmer, K.W. Törnroos, R. Anwander, Europium bis(dimethylsilyl)amides including mixed-valent $Eu_3[N(SiHMe_2)_2]_6[\mu\text{-}N(SiHMe_2)_2]_2$, Dalton Trans. 43 (2014) 17324.
[14] C. Meermann, G. Gerstberger, M. Spiegler, K.W. Törnroos, R. Anwander, Donor and ate-coordination in rare-earth metal bis(dimethylsilyl)amide complexes, Eur. J. Inorg. Chem. (2008) 2014–2023.
[15] H. Schumann, J. Winterfeld, E.C.E. Rosenthal, H. Hemling, L. Esser, Monomere Lanthanoid(III)-amide: Synthese unt Röntgenstrukturanalyse von $[Nd\{N(C_6H_5)(SiMe_3)\}_3(THF)]$, $[Li(THF)_2(\mu\text{-}Cl)_2Nd\{N(C_6H_3Me\text{-}2,6)(SiMe_3)\}_2(THF)]$ und $[ClNd\{N(C6H_3\text{-}iso\text{-}Pr_2\text{-}2,6)(SiMe_3)\}_2(THF)]$, Zeitschrift Anorg. Allg. Chem. 621 (1995) 122.
[16] M. Fang, J.E. Bates, S.E. Lorenz, D.S. Lee, D.B. Rego, J.W. Ziller, F. Furche, W.J. Evans, $(N_2)_3^-$ radical chemistry via trivalent lanthanide salt/alkali metal reduction of dinitrogen: new syntheses and examples of $(N_2)_2^-$ and $(N_2)_3^-$ complexes and density functional theory comparisons of closed shell Sc^{3+}, Y^{3+}, and Lu^{3+}, Inorg. Chem. 50 (2011) 1459.
[17] W.J. Evans, D.S. Lee, D.B. Rego, J.M. Perotti, S.A. Kozimor, E.K. Moore, J.W. Ziller, Expanding dinitrogen reduction chemistry to trivalent lanthanides via the LnZ_3/alkali metal reduction system: evaluation of the generality of forming $Ln_2(\mu\text{-}\eta^2\text{:}\eta^2\text{-}N_2)$ complexes via LnZ_3/K, J. Am. Chem. Soc. 126 (2004) 14574.
[18] M. Fang, D.S. Lee, J.W. Ziller, R.J. Doedens, J.E. Bates, F. Furche, W.J. Evans, Synthesis of the $(N_2)^{3-}$ radical from Y^{2+} and its protonolysis reactivity to form $(N_2H_2)^{2-}$ via the $Y[N(SiMe_3)_2]_3/KC_8$ reduction system, J. Am. Chem. Soc. 133 (2011) 3784.
[19] D.A. Gaul, O. Just, W.S. Rees Jr., Synthesis and characterization of a series of zinc bis[(alkyl)(trimethylsilyl)amide] compounds, Inorg. Chem. 19 (2000) 5648.
[20] I.A. Guzei, M. Wendt, An improved method for the computation of ligand steric effects based on solid angles, Dalton Trans. (2006) 3991.
[21] S.A. Moehring, M.J. Beltrán-Leiva, D. Páez-Hernández, R. Arratia-Pérez, J.W. Ziller, W.J. Evans, Rare-earth metal(II) aryloxides: structure, synthesis, and EPR spectroscopy of $[K(2.2.2\text{-cryptand})][Sc(OC_6H_2{}^tBu_2\text{-}2,6\text{-}Me\text{-}4)_3]$, Chem. Eur. J. 24 (2018) 18059.
[22] C.A.P. Goodwin, K.C. Joslin, S.J. Lockyer, A. Formanuik, G.A. Morris, F. Ortu, I.J. Vitorica-Yrezabal, D.P. Mills, Homoleptic trigonal planar lanthanide complexes stabilized by superbulky silylamide ligands, Organometallics. 34 (2015) 2314.
[23] N. Desmangles, H. Jenkins, K.B. Ruppa, S. Gambarotta, Preparation and characterization of a vanadium (III) dinitrogen complex supported by a tripodal anionic amide ligand, Inorg. Chim. Acta 250 (1996) 1.
[24] D. Rosiak, A. Okuniewski, J. Chojnacki, Novel complexes possessing Hg–(Cl, Br, I)···O=C halogen bonding and unusual $Hg_2S_2(Br/I)_4$kernel. The usefulness of τ_4' structural parameter, Polyhedron 146 (2018) 35.
[25] G. Scarel, C. Wiemer, M. Fanciulli, I.L. Fedushkin, G.K. Fukin, G.A. Domrachev, Y. Lebedinskii, A. Zenkevich, G. Pavia, $[(Me_3Si)_2N]_3Lu$: Molecular structure and use as Lu and Si source for atomic layer deposition of Lu silicate films, Zeitschrift Anorg. Allg. Chem. 633 (2007) 2097.
[26] W.S. Rees Jr., O. Just, D.S. Van Derveer, Materials molecular design of dopant precursors for atomic layer epitaxy of SrS: Ce, J. Mater. Chem. 9 (1999) 249.
[27] P.B. Hitchcock, A.G. Hulkes, M.F. Lappert, Z. Li, Cerium(III) dialkyl dithiocarbamates from $[Ce\{N(SiMe_3)_2\}_3]$ and tetraalkylthiuram disulfides, and $[Ce(\kappa^2\text{-}S_2CNEt_2)_4]$ from the Ce^{III} precursor; Tb^{III} and Nd^{III} analogues, Dalton Trans. (2004).
[28] W.A. Herrmann, R. Anwander, F.C. Munck, W. Scherer, V. Dufaud, N.W. Huber, G.R.J. Artus, I.X. Lanthanoiden-Komplexe, [1] Reaktivitätsbestimmender Einfluß der Ligandenkonstitution bei Seltenerdamiden: Herstellung und Struktur sterisch überladener Alkoxid-Komplexe, Zeitschrift Naturforsch. B 49b (1994) 1789.
[29] E. Sheng, G. Yang, B. Dong, Synthesis and crystal structure of three coordinate planar neodymium amide $[(Me_3Si)_2N]_3Nd$, J. Anhui Norm. Univ. (Natural Sci.) (2002) 254.
[30] M. Westerhausen, M. Hartmann, A. Pfitzner, W. Schwarz, Bis(trimethylsilyl) amide und -methanide des Yttriums – Molekulstrukturen von Tris (diethylether-O)lithium-(μ-chloro)-tris[bis(trimethylsilyl)methyl]yttriat, solvensfreiem Yttrium-tris[bis(trimethylsilyl)amid] sowie dem Bis (benzonitril)-Komplex, Zeitschrift Anorg. Allg. Chem. 621 (1995) 837.
[31] R.D. Shannon, Revised effective ionic radii and systematic studies of interatomic distances in halides and chalcogenides, Acta Crystallogr., Sect. A 32 (1976) 751.
[32] N.C. Boyde, S.C. Chmely, T.P. Hanusa, A.L. Rheingold, W.W. Brennessel, Structural distortions in $M[E(SiMe_3)_2]_3$ complexes (M = Group 15, f-element; E = N, CH): is three a crowd?, Inorg Chem. 53 (2014) 9703.
[33] D.H. Woen, G.P. Chen, J.W. Ziller, T.J. Boyle, F. Furche, W.J. Evans, Solution synthesis, structure, and CO2 reduction reactivity of a scandium(II) complex, $\{Sc[N(SiMe_3)_2]_3\}^-$, Angew. Chem., Int. Ed. 56 (2017) 2050.
[34] E.D. Brady, D.L. Clark, J.C. Gordon, P.J. Hay, D.W. Keogh, R. Poli, B.L. Scott, J.G. Watkin, Tris(bis(trimethylsilyl)amido)samarium: X-ray structure and DFT study, Inorg. Chem. 42 (2003) 6682.
[35] M. Niemeyer, Synthesis and structural characterization of several ytterbium bis(trimethylsilyl)amides including base-free $[Yb\{N(SiMe_3)_2\}_2(\mu\text{-}Cl)]_2$ — a coordinatively unsaturated complex with additional agostic Yb···(H$_3$C—Si) interactions, Zeitschrift Anorg. Und Allg. Chem. 628 (2002) 647.
[36] W.A. Hermann, R. Anwander, F.C. Munch, W. Scherer, V. Dufaud, N.W. Huber, G.R.J. Artus, I.X. Lanthanoiden-Komplexe, [1] Reaktivitätsbestimmender Einfluß der Ligandenkonstitution bei Seltenerdamiden: Herstellung und Struktur sterisch überladener Alkoxid-Komplexe, Zeitschrift Naturforsch. 49b (1994) 1789.
[37] M. Sugiura, S. Kobayashi, T. Ollevier, Scandium trifluoromethanesulfonate, in: Encyclopedia of Reagents for Organic Synthesis, John Wiley & Sons, Ltd, 2015. https://onlinelibrary.wiley.com/doi/10.1002/047084289X.rn00165.pub2.
[38] C. Schädle, C. Meermann, K.W. Törnroos, R. Anwander, Rare-earth Metal Phenyl(trimethylsilyl)amide Complexes, Eur. J. Inorg. Chem. (2010) 2841–2852.
[39] C.A.P. Goodwin, N.F. Chilton, G.F. Vettese, E.M. Pineda, I.F. Crowe, J.W. Ziller, R. E.P. Winpenny, W.J. Evans, D.P. Mills, physicochemical properties of near-linear lanthanide(II) bis(silylamide) complexes (Ln = Sm, Eu, Tm, Yb), Inorg. Chem. 55 (2016) 10057.
[40] P.B. Hitchcock, M.F. Lappert, L. Maron, A.V. Protchenko, Lanthanum does form stable molecular compounds in the +2 oxidation state, Angew. Chem., Int. Ed. 47 (2008) 1488.
[41] N.F. Chilton, C.A.P. Goodwin, D.P. Mills, R.E.P. Winpenny, The first near-linear bis(amide) f-block complex: a blueprint for a high temperature single molecule magnet, Chem. Commun. 51 (2015) 101.
[42] F.P. Gabbaï, P.J. Chirik, D.E. Fogg, K. Meyer, D.J. Mindiola, L.L. Schafer, S.L. You, An editorial about elemental analysis, Organometallics 35 (2016) 3255.